THE JOURNAL OF BIOLOGICAL CHEMISTRY
Vol. 273, No. 15, Issue of April 10, pp. 8659–8668, 1998

Printed in U.S.A.

Probing the Structure of the Nicotinic Acetylcholine Receptor Ion Channel with the Uncharged Photoactivable Compound [^{3}H]Diazofluorene*

(Received for publication, November 25, 1997, and in revised form, January 22, 1998)

Michael P. Blanton‡§, Lawrence J. Dangott‡, S. K. Raja¶, Anil K. Lala¶, and Jonathan B. Cohen‡‖

From the ‡Department of Neurobiology, Harvard Medical School, Boston, Massachusetts 02115 and ¶Biomembrane Lab, Department of Chemistry, Indian Institute of Technology Bombay, Powai, Bombay 400076, India

The uncharged photoactivable probe 2-[^{3}H]diazofluorene ([^{3}H]DAF) was used to examine structural changes in the *Torpedo californica* nicotinic acetylcholine receptor (AChR) ion channel induced by agonists. Photoincorporation of [^{3}H]DAF into the AChR consisted of the following two components: a nonspecific component consistent with incorporation into residues situated at the lipid-protein interface, and a specific component, inhibitable by noncompetitive antagonists and localized to the M2 hydrophobic segments of AChR subunits. The nonspecific [^{3}H]DAF incorporation was characterized in the M4 segment of each AChR subunit. The observed distribution and periodicity of labeled residues reinforce the conclusion that the M4 segments are organized as transmembrane α-helices with a common "face" of each helix in contact with lipid. Within the M2 segments, in the absence of agonist [^{3}H]DAF specifically labeled homologous residues βVal-261 and δVal-269, with incorporation into δVal-269 at a 5-fold greater efficiency than into βVal-261. This observation, coupled with the lack of detectable incorporation into α-M2 including the homologous αVal-255, indicates that within the resting channel [^{3}H]DAF is bound with its photoreactive diazo group oriented toward δVal-269. In the presence of agonist, there is an ~90% reduction in the labeling of βVal-261 and δVal-269 accompanied by specific incorporation into residues (βLeu-257, βAla-258, δSer-262, and δLeu-265) situated 1 or 2 turns of an α-helix closer to the cytoplasmic end of the M2 segments. The results provide a further characterization of agonist-induced rearrangements of the M2 (ion channel) domain of the AChR.

The nicotinic acetylcholine receptor (AChR)[1] isolated from the electric organ of the marine elasmobranch *Torpedo californica* is the best characterized member of a family of ligand-gated ion channels which includes the γ-aminobutyric acid, glycine, and serotonin 5-HT$_3$ receptors (for recent reviews, see Refs. 1–3). The AChR is composed of four homologous subunits ($\alpha_2\beta\gamma\delta$) arranged quasi-symmetrically around a central cation-selective ion channel (4). The subunits each have a characteristic topology as follows: a large hydrophilic N-terminal domain containing the agonist binding sites, followed in the primary structure by three hydrophobic membrane-spanning segments (M1–M3), a cytoplasmic domain, a fourth hydrophobic transmembrane segment (M4), and a short extracellular C-terminal tail.

Noncompetitive antagonists (NCAs) are agents that block the AChR permeability response without binding to the agonist site. These compounds are structurally diverse and include many aromatic amines but also general anesthetics, steroids, and even the neuropeptide substance P (reviewed in Ref. 5). A number of NCAs have been instrumental in identifying regions of the AChR which contribute to the formation of the pore of the ion channel. Photoaffinity labeling studies with [^{3}H]chlorpromazine (6–9) and [^{3}H]triphenylmethylphosphonium (10) as well as reaction with [^{3}H]meproadifen mustard (11) have all identified labeled residues within the M2 segments that would all lie on a common side of an α-helix. These results, in conjunction with the observed functional properties of AChRs with mutations in the M2 segments (1, 2), provide the basis for a model of the ion channel comprised of M2 segments of each subunit arranged as transmembrane α-helices around the central axis, a model consistent with studies of AChR three-dimensional structure derived from electron micrographic image analysis (4, 12).

The sites of [^{3}H]chlorpromazine, [^{3}H]triphenylmethylphosphonium, and [^{3}H]meproadifen mustard incorporation were all identified in the presence of agonist under conditions where the AChR is expected to be in the desensitized state. More recently, 3-(trifluoromethyl)-3-(*m*-[^{125}I]iodo-phenyl)diazirine ([^{125}I]TID), a small, uncharged photoactivable probe, was used to identify residues in the channel lining M2 region both in the absence and presence of agonist, *i.e.* for AChRs predominantly in the resting state or desensitized state, respectively (13). [^{125}I]TID is a potent NCA (14, 15) that reacts nonspecifically with AChR amino acids in M3 and M4 hydrophobic segments at the lipid-protein interface (14–17) and specifically with amino acids in M2 segments of each AChR subunit (13). In the absence of agonist (resting state), [^{125}I]TID labeled δLeu-265 and δVal-269 and the homologous residues in the other subunits that are located 9 and 13 amino acids to the C-terminal side of the conserved lysine residue at the N terminus of the M2 region (positions 9 and 13). In the desensitized state, the pattern of [^{125}I]TID-labeled residues broadened to include homologous serine residues at positions 2 and 6 (*i.e.* δSer-258 and δSer-

* This work was supported in part by United States Public Health Service Grants NS 19522 and GM 15904 (to J. B. C.) and by an award in Structural Neurobiology from the Keck Foundation. The costs of publication of this article were defrayed in part by the payment of page charges. This article must therefore be hereby marked "*advertisement*" in accordance with 18 U.S.C. Section 1734 solely to indicate this fact.

§ Present address: Dept. of Pharmacology, Texas Tech Univ. Health Sciences Center, Lubbock, TX 79430.

‖ To whom correspondence should be addressed: Dept. of Neurobiology, Harvard Medical School, 220 Longwood Ave., Boston, MA 02115. Tel.: 617-432-1728; Fax: 617-734-7557; E-mail:jbcohen@warren.med.harvard.edu.

[1] The abbreviations used are: AChR, nicotinic acetylcholine receptor; 1-AP, 1-azidopyrene; [^{3}H]DAF, 2-[^{3}H]diazofluorene; [^{125}I]TID, 3-trifluoromethyl-3-(-*m*-[^{125}I]iodophenyl) diazirine; PAGE, polyacrylamide gel electrophoresis; HPLC, high performance liquid chromatography; EKC, endoproteinase Lys-C; PCP, phencyclidine; PTH, phenylthiohydantoin; NCAs, noncompetitive antagonists; Tricine, *N*-[2-hydroxy-1,1-bis(hydroxymethyl)ethyl]glycine.

262). These results provided the first direct evidence of an agonist-induced structural rearrangement of the channel lining M2 helices. They further suggested that in the closed ion channel the aliphatic residues at positions 9 and 13 form a permeability barrier to the passage of ions.

To examine further the structure of the channel in different functional states, we examined the incorporation into the AChR of another lipophilic photoactivable probe, [^{3}H]diazofluorene ([^{3}H]DAF), both in the absence and presence of agonist. [^{3}H]DAF has been used to probe the hydrophobic core of erythrocyte membranes (18) as well as the sites of lipid exposure of *Staphylococcus aureus* α-toxin (19). Whereas incorporation of [^{125}I]TID and [^{3}H]DAF both proceed through a UV-induced reactive carbene, the two compounds are structurally distinct, and TID produces a singlet carbene (20) whereas DAF produces a carbene with substantial triplet character (21, 22). We report here that like [^{125}I]TID, [^{3}H]DAF not only incorporates into residues situated at the lipid-protein interface but also into residues in the channel lining M2 segments. We identify the amino acids within the M4 segments that are labeled nonspecifically as well as the pattern of specific photoincorporation within the M2 segments. The subunit selectivity of photolabeling within the M2 domain in conjunction with the agonist-dependent redistribution of labeling provide further information about the change in structure of the AChR ion channel domain between resting and desensitized states.

EXPERIMENTAL PROCEDURES

Materials—AChR-rich membranes were isolated from *T. californica* electric organ (17). 2-[^{3}H]Diazofluorene ([^{3}H]DAF) of specific activities ranging from 0.67 to 1.4 Ci/mmol was prepared from 2-[^{3}H]fluorenone according to the procedure described by Pradhan and Lala (18), repurified, and stored at −20 °C in ethanol. [^{3}H]Phencyclidine (43 Ci/mmol) was from NEN Life Science Products, and [^{3}H]tetracaine (47 Ci/mmol) was prepared at NEN Life Science Products by catalytic tritiation of 3,3-dibromotetracaine. 1-Azidopyrene was purchased from Molecular Probes. Carbamylcholine and tetracaine were from Sigma, and phencyclidine (PCP) was from Alltech Associates. L-1-Tosylamido-2-phenylethyl chloromethyl ketone-treated trypsin was purchased from Worthington and endoproteinase Lys-C from Boehringer Mannheim. Genapol C-100 (10%) was purchased from Calbiochem. Prestained low molecular weight gel standards were purchased from Life Technologies, Inc.

Photolabeling AchR-rich Membranes with [^{3}H]DAF—For analytical labeling experiments, *Torpedo* membranes (2 mg/ml) in *Torpedo* physiological saline (TPS, 250 mM NaCl, 5 mM KCl, 3 mM $CaCl_2$, 2 mM $MgCl_2$, 5 mM sodium phosphate, pH 7.0) were incubated with [^{3}H]DAF at a final concentration of 5 μM in the absence or presence of 100 μM carbamylcholine and in the absence or presence of additional ligands. After a 30-min incubation, suspensions were irradiated for 5 min at a distance of less than 1 cm with a 365-nm lamp (EN-Spectroline). Following irradiation, each sample was pelleted (15,000 × *g*), the pellet solubilized in sample loading buffer (23), and then submitted to SDS-PAGE. Preparative photolabelings (12–15 mg per condition) were carried out at 10 μM [^{3}H]DAF (±100 μM tetracaine) and in the presence of carbamylcholine (±100 μM phencyclidine). After 1 h incubation, sequential photoincorporation of [^{3}H]DAF and then 1-azidopyrene (1-AP) was carried out as described previously for [^{125}I]TID (17), except that irradiation of suspensions with 1-AP was limited to 5 min. Samples were then pelleted and solubilized in electrophoresis sample loading buffer and submitted to SDS-PAGE.

SDS-Polyacrylamide Gel Electrophoresis—SDS-PAGE was performed as described by Laemmli (23) using either 1.0-mm (analytical) or 1.5-mm (preparative scale) thick 8% polyacrylamide gels with 0.33% bis(acrylamide). For analytical gels, polypeptides were visualized by staining with Coomassie Blue R-250 (0.25% w/v in 45% methanol and 10% acetic acid) and destaining in 25% methanol, 10% acetic acid. The gels were then impregnated with fluor (Amplify, Amersham Pharmacia Biotech) for 20 min with rapid shaking, dried, and exposed at −80 °C to Kodak X-OMAT LS film for various times (3–12 weeks). Incorporation of ^{3}H into individual polypeptides was quantified by scintillation counting of excised gel pieces as described (24). For preparative scale gels, polypeptides incorporating 1-AP were visualized from their associated fluorescence when the gels were illuminated at 365 nm on a UV-light box. Bands corresponding to AChR subunits were excised, and in some cases the gel pieces were transferred to the wells of individual 15% mapping gels (25, 26). Mapping gels were composed of a 4.5% acrylamide stacking gel and a 15% acrylamide separating gel. The gel pieces were overlaid with 350 μl of buffer (5% sucrose, 125 mM Tris-HCl, 0.1% SDS, pH 6.8) containing 250 μg of *S. aureus* V8 protease (500 μg V8 protease for gel pieces containing the α-subunit). Electrophoresis was carried out overnight at 25 mA constant current. In the course of this work it was determined that for membranes labeled with 1-AP and [^{3}H]DAF, the fluorescent- and ^{3}H-labeled-AChR subunits comigrated, as did their large proteolytic fragments.

1-AP/[^{3}H]DAF-labeled subunits and proteolytic fragments were isolated from the excised gel pieces using a passive elution protocol (17, 27). The eluate was filtered (Whatman No. 1), and the protein was concentrated using a Centriprep-10 (Amicon). Excess SDS was removed by acetone precipitation (overnight at −20 °C).

Purification of Proteolytic Digests of [^{3}H]DAF/1-AP-labeled AChR Subunits to Isolate Fragments Containing the M2 Segment—For trypsin digestion, acetone-precipitated subunits (β and δ) were resuspended in a small volume (~50 μl) of buffer (100 mM NH_4HCO_3, 0.1% SDS, pH 7.8). The SDS concentration was then reduced by diluting with buffer without SDS, and Genapol C-100 was added, resulting in final concentrations of 0.02% SDS, 0.5% Genapol C-100, and 1–2 mg/ml protein. Trypsin was added to a 1:5 (w/w) enzyme to substrate ratio and incubated at room temperature for 4 days. For endoproteinase Lys-C (EKC) digestion, subunits (α) were resuspended in 15 mM Tris-HCl, 0.1% SDS, pH 8.1, at 1–2 mg/ml protein. Approximately 1.5 units of EKC was added and incubated at room temperature for 6 days. Both trypsin and EKC digests were separated on Tricine/SDS-polyacrylamide gels prepared as described (17, 28). Aliquots of each of the digests (~5%) were routinely resolved on analytical scale Tricine/SDS-polyacrylamide gels (1.0-mm thick) along with prestained molecular weight standards (Life Technologies, Inc.) as follows: ovalbumin (43,000), carbonic anhydrase (29,000), α-lactoglobulin (18, 400), lysozyme (14, 300), bovine trypsin inhibitor (6, 200), the A chain of insulin (3, 400), and the B chain of insulin (2, 300). Analytical gels were soaked in 25% methanol, 10% acetic acid for 30 min, and then prepared for fluorography.

For each of the AChR subunits labeled under a given condition, the bulk of the proteolytically digested material was resolved on individual 1.5-mm thick Tricine/SDS-polyacrylamide gels. Proteolytic fragments containing the M2 region of each of the AChR subunits were identified and isolated using two different sets of criteria. First, for digestion conditions nearly identical to those employed here, it had been determined previously where proteolytic fragments containing the M2 segments migrate relative to Life Technologies, Inc., pre-stained molecular weight standards (11, 13). Second, proteolytic fragments were selected which begin at the N termini of the M2 segments and extend through M3 hydrophobic segments. Incorporation of 1-AP into the M3 segments (17) could then be used to visualize the M2-M3 fragment by illuminating the Tricine/SDS-polyacrylamide gel at 365 nm on a UV-light box. Finally, aliquots of each of the digests were resolved on analytical Tricine/SDS-polyacrylamide gels, and some time later, fluorographs of those gels were used to confirm that [^{3}H]DAF was indeed incorporated into these bands.

1-AP/[^{3}H]DAF-labeled fragments were further purified by reversed-phase HPLC using a Brownlee Aquapore C_4 column (100 × 2.1 mm) as described (17). Solvent A was 0.08% trifluoroacetic acid in water; solvent B was 0.05% trifluoroacetic acid in 60% acetonitrile, 40% 2-propanol, and the elution gradient was from 25 to 100% solvent B in 80 min. The elution of peptides was monitored by the absorbance at 210 nm and by fluorescence emission (357 nm excitation, 432 nm emission). The elution of [^{3}H]DAF was monitored by scintillation counting of an aliquot (25 μl) of each fraction.

Generation and Isolation of Fragments of AChR Subunits Containing [^{3}H]DAF/1-AP-labeled M4 Segments—Fragments beginning near the N terminus of the M4 segment of each AChR subunit were isolated as described (17) for [^{125}I]TID/1-AP-labeled subunits. Briefly, in gel digestion of each isolated subunit with *S. aureus* V8 protease was used to generate 10–14-kDa subunit fragments as follows: αV8–10 (αAsn-339 to αGly-437); βV8–12 (βMet-384/βSer-417 to βAla-469); γV8–14 (γLeu-373/γIle-413 to γPro-489; δV8–11 (Lys-δ436 to δAla-501). Trypsin digests of these fragments were fractionated by Tricine/SDS-PAGE yielding fluorescent and ^{3}H containing bands of 3–4 kDa for α-subunit (αT-4K), 5 kDa for β- and γ-subunits (βT-5K and γT-5K), and 6 kDa for δ-subunit (δT-6K). Material eluted from these bands was further purified by reversed-phase HPLC. With the exception of the δ-subunit digest, each digest yielded a single major peak of ^{3}H which coeluted with 1-AP fluorescence, and these peaks eluted at the same concentra-

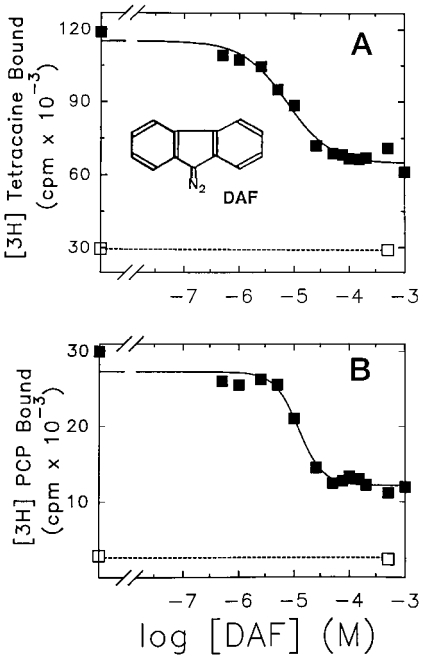

FIG. 1. **Effects of diazofluorene on the binding of [^{3}H]tetracaine and [^{3}H]PCP in the absence and in the presence of carbamylcholine, respectively.** AChR-rich membranes (0.5 mg/ml, 0.60 μM ACh binding sites) containing 2 nM [^{3}H]tetracaine (*A*) or 6 nM [^{3}H]PCP and 200 μM carbamylcholine (*B*) were equilibrated for 2–3 h with increasing concentrations of diazofluorene (*DAF*). Bound tritiated ligand (■) was determined by centrifugation ("Experimental Procedures"). In each panel the *dashed line* indicates nonspecific bound tritiated ligand in the presence of 200 μM tetracaine (*A*, □) or meproadifen (*B*, □) at 0 and 500 μM DAF.

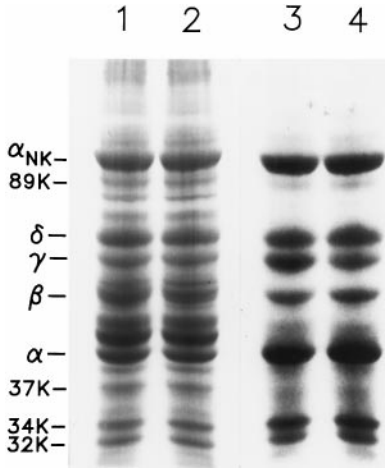

FIG. 2. **Photoincorporation of [^{3}H]DAF into AChR-rich membranes in the absence and presence of carbamylcholine.** AChR-rich membranes were equilibrated with [^{3}H]DAF (5 μM) in the absence (*lanes 1* and *3*) and in the presence (*lanes 2* and *4*) of 100 μM carbamylcholine and irradiated at 365 nm for 5 min. Polypeptides were resolved by SDS-PAGE, visualized by Coomassie Blue stain (*lanes 1* and *2*), and processed for fluorography (4-week exposure; *lanes 3* and *4*). Labeled lipid and free photolysis products were electrophoresed from the gel with the tracking dye. The AChR subunits and the Na^+/K^+ ATPase α-subunit (α_{NK}) are indicated. In addition, bands of 89 (*89K*), 37 (*37K*), 34 (*34K*), and 32 (*32K*) kDas are also indicated. These bands have been identified by N-terminal sequence analysis of purified proteolytic fragments to be the chloride channel CLC-0, calectrin (annexin V), the mitochondrial voltage-dependent anion channel, and the mitochondrial ATP/ADP translocase, respectively. The AChR-associated 43-kDa protein is not indicated but can be seen migrating with a slightly slower mobility than the AChR α-subunit (*lanes 1* and *2*). Also not indicated is a 105-kDa band that can be seen migrating with slightly slower mobility than the α-subunit of the Na^+/K^+ ATPase.

tions of organic solvent as had been seen for the [^{125}I]TID/1-AP-labeled M4 segments. Material in these fractions were pooled, dried, and resuspended for protein microsequence analysis. The tryptic digest of δT-6K yielded a broader distribution of ^{3}H without significant fluorescence, and material was pooled from the concentrations of organic eluent that had been found to contain [^{125}I]TID/1-AP-labeled δM4.

Sequence Analysis—N-terminal sequence analysis was performed on an Applied Biosystems model 477A protein sequencer using gas phase cycles. Pooled HPLC samples were dried by vacuum centrifugation, resuspended in a small volume of 0.05% SDS (~20 μl), and immobilized on chemically modified glass fiber disks (Beckman Instruments). Approximately 30% of the released PTH-derivatives were separated by an on-line Model 120A PTH-derivative analyzer, and approximately 60% was collected for determination of released ^{3}H by scintillation counting of each sample for three 5-min intervals. Initial yield (I_0) and repetitive yield (R) were calculated by nonlinear least squares regression of the observed release (M) for each cycle (n): $M = I_0R^n$ (PTH-derivatives of Ser, Thr, Cys, and His were omitted from the fit).

Radioligand Binding Assays—The equilibrium binding of [^{3}H]PCP (6 nM), [^{3}H]tetracaine (2 nM), and [^{3}H]histrionicotoxin (10 nM) to *Torpedo* membranes was assayed by centrifugation. 500-μl aliquots of membrane suspensions (0.5 mg of protein/ml in TPS, ~0.6 μM AChR) were equilibrated with the radioligand and the nonradioactive cholinergic ligands for 2–3 h in 10 × 75-mm Pyrex disposable culture tubes (Corning) and then transferred to 1.5-ml plastic microcentrifuge tubes and pelleted for 45 min at 15,000 rpm in a Sorvall SA-600 rotor. After removal of the supernatants, the membrane pellets were solubilized in 100 μl of 10% SDS, and the pellet ^{3}H was determined by liquid scintillation counting.

RESULTS

In initial experiments, nonradioactive DAF (Fig. 1) was tested as an inhibitor of the equilibrium binding of radiolabeled, positively charged AChR NCAs. [^{3}H]Tetracaine binds with high affinity (K_{eq} = 0.3 μM) in the absence of agonist to one site per AChR monomer, whereas it binds ~100-fold more weakly to desensitized AChRs (29). The sites of specific photoincorporation of [^{3}H]tetracaine are restricted to amino acids within each M2 segment (30). In the absence of agonist, DAF produced a dose-dependent inhibition of [^{3}H]tetracaine binding (IC_{50} = 6 μM), with high concentrations inhibiting ~60% of specific binding[2] (Fig. 1*A*). For desensitized AChRs, [^{3}H]phencyclidine binds with high affinity (K_{eq} = 1 μM) to a single site per AChR (31), and DAF also acted as an allosteric inhibitor of [^{3}H]phencyclidine binding (Fig. 1*B*, IC_{50} = 10 μM, 60% maximal inhibition). DAF also acted as an allosteric inhibitor of [^{3}H]histrionicotoxin binding, with IC_{50} = 2 μM and maximal inhibition of 50% in the presence of agonist (data not shown).

Initial photolabeling experiments were designed to characterize the general pattern of [^{3}H]DAF photoincorporation into *Torpedo* AChR-rich membranes as well as to test the sensitivity of the photoincorporation to cholinergic ligands. Membranes (2 mg/ml) were equilibrated with 5 μM [^{3}H]DAF in the absence and in the presence of 100 μM carbamylcholine. After irradiation, membrane suspensions were pelleted and resuspended in electrophoresis sample buffer, and the pattern of incorporation was monitored by SDS-PAGE followed by fluorography. As is evident in the fluorograph of an 8% polyacrylamide gel (Fig. 2, *lanes 3* and *4*), there was appreciable incorporation of [^{3}H]DAF into each of the AChR subunits. Neither the overall labeling pattern nor the relative incorporation into individual AChR subunits was affected by the inclusion of 100 μM carbamylcholine (Fig. 2, *lane 4*). Based on liquid scintillation counting of excised gel bands, ~1% of subunits incorporated ^{3}H, with approximately equal incorporation in each subunit ($\alpha/\beta/\gamma/\delta$: 1/(0.8 ± 0.2)/(0.93 ± 0.3)/(1.2 ± 0.3)). The presence of carba-

[2] Although high concentrations of DAF were apparently unable to fully displace [^{3}H]PCP or [^{3}H]tetracaine, further studies are required to determine whether this reflects a true allosteric inhibition or the limited aqueous solubility of DAF.

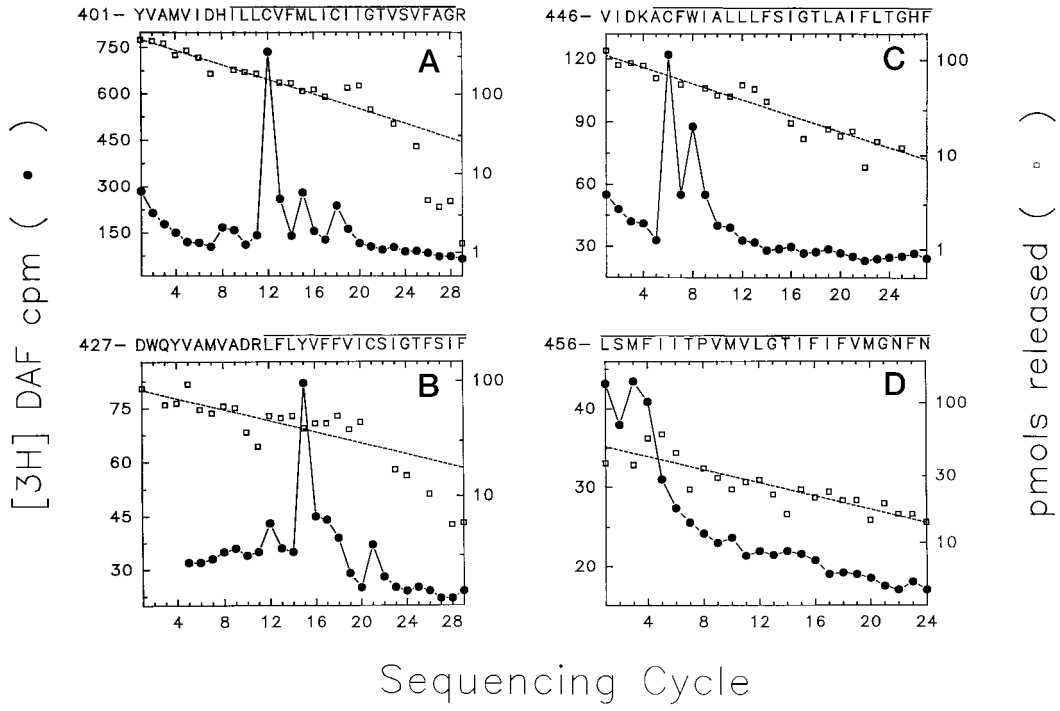

FIG. 3. **Radioactivity and mass release upon sequential Edman degradation of [^{3}H]DAF/1-AP-labeled fragments containing the M4 segment.** *A*, α-subunit tryptic peptide T-4K isolated by HPLC from membranes labeled with 5 μM [^{3}H]DAF (18,800 cpm loaded on the filter and 3,770 cpm remaining after 29 cycles). The only sequence detected began at αTyr-401 (I_0, 490 pmol; *R*, 90%). *B*, β-subunit tryptic peptide T-5K isolated by HPLC (3,480 cpm loaded on the filter and 591 cpm remaining after 29 cycles). The primary sequence began at βAsn-427 before M4 (I_0, 85 pmol; *R*, 95%), with a secondary sequence beginning at αTyr-401 before α-M4 (I_0, 24 pmol; *R*, 91% (see text[3])). *C*, γ-subunit tryptic fragment T-5K isolated by HPLC (3,680 cpm loaded on the filter and 669 cpm remaining after 27 cycles). The only sequence detected began at γVal-446 (I_0, 110 pmol; *R*, 91%). *D*, δ-subunit tryptic peptide T-6K isolated by HPLC (1,660 cpm loaded on the filter and 290 cpm remaining after 24 cycles). The only sequence detected began at δLeu-456 (I_0, 49 pmol; *R*, 95%). For each sample 60% of each cycle of Edman degradation was analyzed for released ^{3}H (●) and 30% for PTH-derivatives (□), with the *dashed lines* corresponding to the exponential decay fit of the amount of detected PTH-derivatives for the peptides containing M4. The amino acid sequence of the sequenced peptide containing the M4 region is shown *above* each panel, with the *solid line* indicating the limits of the M4 regions.

mylcholine resulted in a <10% change of subunit labeling. Incorporation of [^{3}H]DAF into the AChR subunits accounted for approximately 60% of the total labeling in polypeptides present in *Torpedo* AChR-rich membranes.

Two NCAs, tetracaine and proadifen, were tested at concentrations of 3, 30, and 250 μM for their effects on [^{3}H]DAF photoincorporation into AChR-rich membranes in the absence and in the presence of 100 μM carbamylcholine, respectively. The effects of these ligands on [^{3}H]DAF (5 μM) photoincorporation was examined by fluorography and by liquid scintillation counting of excised gel pieces. The pattern of incorporation was qualitatively very similar in each of the different conditions, with a small dose-dependent decrease (~15–25%) in the labeling of the subunits evident for both tetracaine and proadifen that was not seen for other labeled non-AChR polypeptides (data not shown). The relative distribution of ^{3}H incorporation within the α-subunit was examined by determining ^{3}H incorporation within the four large, non-overlapping α-subunit fragments that can be generated by digestion with *S. aureus* V8 protease (14, 26). Inspection of the fluorograph of the dried mapping gel indicated that all the visible labeling was contained within a 20-kDa fragment (αV8–20, Ser-173–Glu-338) containing hydrophobic segments M1–M3 and a 10-kDa fragment (αV8–10, Asn-339–Gly-437) containing the M4 segment. Based on liquid scintillation counting of the excised gel pieces, 75% of ^{3}H cpm was incorporated in αV8–10 and 25% was in αV8–20, with the relative incorporation of [^{3}H]DAF into αV8–10 similar for labelings carried out in the absence (77%) and in the presence (74%) of 100 μM carbamylcholine.

Sites of [^{3}H]DAF Incorporation in M4 Segments of Each AChR Subunit—The M4 segments were isolated from tryptic digests of large V8-protease fragments of each of the receptor subunits as described under "Experimental Procedures." For α-subunit, tryptic digestion of αV8–10 produced a fluorescent and radioactive band of 3–4 kDa (αT-4K), which was further purified by reversed-phase HPLC. N-terminal sequence analysis (Fig. 3*A*) revealed the presence of a single sequence beginning at αTyr-401 (490 pmol) that was present in a 10–20-fold greater abundance than any secondary sequence. The largest release of ^{3}H occurred in cycle 12, with additional release in cycles 8, 15, and 18. The same pattern of ^{3}H release was seen for the M4 segment isolated from membranes labeled in the presence of 100 μM carbamylcholine (data not shown). ^{3}H release in cycle 12 indicated that αCys-412 was the primary site of incorporation of [^{3}H]DAF in αM4, as it was for [^{125}I]TID (17), with lower level reaction with αHis-408, αMet-415, and αCys-418.

Tryptic digestion of βV8–12 produced a fluorescent and radioactive band migrating with an apparent molecular mass of 5 kDa (βT-5K) on a Tricine/SDS-polyacrylamide gel which was further purified by HPLC. As shown in Fig. 3*B*, sequence analysis of this material revealed the presence of a primary sequence beginning at βAsp-427 (84 pmol), as well as a secondary sequence beginning at Tyr-401 of the α-subunit (24 pmol).[3]

[3] The presence of a contaminating α-subunit fragment in β-subunit fractions occurred uniquely in the particular experiment in Fig. 3*B*. Since α-subunit does not contaminate β-subunit preparations in detectable quantities, the contamination in this sample most likely resulted when the reversed-phase HPLC column was washed insufficiently between the purification of the α-subunit T-4K fragment and the purification of the β-subunit T-5K band. Based upon an estimated 8.6 pmol of αCys-412 in cycle 12 of the β-subunit sample (Fig. 3*B*, calculated from

The largest ^{3}H release occurred in cycle 15, with additional release in cycles 12 and 21 and a "shoulder" of release in cycles 17 and 18. The amount of αTyr-401 peptide present was clearly insufficient to account for the release in cycles 15, 17, 18, and 21, although it did account[3] for the release in cycle 12. Therefore, a comparison of the pattern of ^{3}H release with the corresponding amino acids identified in the peptide beginning at βAsp-427 indicate that Tyr-441 is the primary site of labeling, with additional reaction with Phe-443, Phe-444, and Cys-447. When the M4 region was isolated from membranes labeled in the presence of 100 μM carbamylcholine and the purified material then subjected to sequence analysis, a single sequence was detected beginning at βAsp-427 (34 pmol) and the same four residues were found to be labeled, with no release detected in cycle 12.

When the tryptic digest of γV8–14 was resolved on a Tricine/SDS-polyacrylamide gel, a band of fluorescence and ^{3}H migrated with an apparent molecular mass of 5 kDa (γT-5K) which was eluted and further purified by reversed-phase HPLC. Sequence analysis (Fig. 3*C*) revealed the presence of a single sequence beginning at γVal-446 and extending through γM4 (112 pmol), with ^{3}H release in cycles 6 and 8 consistent with [^{3}H]DAF incorporation into γCys-451 and γTrp-453 within γ-M4. ^{3}H incorporation into these two residues was also seen in the N-terminal sequence analysis of γT-5K isolated from membranes labeled in the presence of carbamylcholine (not shown).

The tryptic digest of δV8–11 produced a faint band of fluorescence and ^{3}H which migrated with an apparent molecular mass of 6 kDa (δT-6K). The HPLC elution profile of the material isolated from the δT-6K band exhibited a broad and complex distribution of ^{3}H which included a peak eluting at the concentration of organic solvent characteristic of the elution of [^{125}I]TID-labeled δ-M4 (17). Sequence analysis of this material (Fig. 3*D*) established the presence of a single sequence beginning at δLeu-456 (49 pmol). Thus, for δV8–11, trypsin cleaved after Arg-455 at the beginning of M4, even though for the corresponding γ-subunit fragment efficient cleavage occurred not at the corresponding γLys-449 but at the preceding γLys-445. No clear ^{3}H release was detected above the general washoff of ^{3}H in the early cycles, although there was very small release of ^{3}H (5 cpm) detected in cycles 3 and 4 corresponding to δMet-458 and δPhe-459. Similar low level release (8 cpm) was also detected in cycle 4, with no release above background in cycle 3, when this δ-M4 peptide was isolated in another experiment from membranes labeled in the presence of 100 μM carbamylcholine.

[^{3}H]DAF Labeling in the Ion Channel—To determine the sites, the agonist sensitivity, and the specificity of [^{3}H]DAF photoincorporation in the M2 regions of AChR subunits, *T. californica* AChR-rich membranes (~1.4 μM AChR) were photolabeled with 10 μM [^{3}H]DAF under four different conditions as follows: 1) in the absence of agonist; 2) in the absence of agonist and in the presence of 100 μM tetracaine; 3) in the presence of 100 μM carbamylcholine; 4) in the presence of 100 μM carbamylcholine and in the presence of 100 μM phencyclidine (PCP).

Identification of the Sites of [^{3}H]DAF Incorporation in δ-M2—The δ-subunits isolated from AChRs labeled with [^{3}H]DAF under the four different conditions (~300 μg/condition) were digested with 20% (w/w) trypsin for 4 days. The digests were resolved by Tricine/SDS-PAGE, and a 5.1-kDa fragment (δT-5.1K; Fig. 4), known to contain the M2-M3 region (13), was isolated from the gel as described under "Experimental Procedures." The material eluted from the δT-5.1K band was further purified by reversed-phase HPLC (Fig. 5), and for each labeling condition, the majority of ^{3}H counts eluted in a peak centered at 74% solvent B. HPLC fractions 29–31 were pooled and sequenced (Fig. 6). For each of the labeling conditions, a single sequence was evident beginning at δMet-257 at the N terminus of δ-M2. In addition, each of the samples sequenced with similar efficiencies and mass levels (see legend to Fig. 6). For δT-5.1K labeled in the absence of agonist, ^{3}H release occurred primarily in cycle 13 (Fig. 6*A* (●)), a result that indicates that the labeled amino acid is δVal-269 (26 cpm/pmol) in δ-M2. For the ^{3}H release profile of δT-5.1K labeled in the absence of agonist but in the presence of 100 μM tetracaine (○, Fig. 6*A*), there was an approximately 90% reduction in [^{3}H]DAF incorporation into δVal-269 (3 cpm/pmol). The presence of agonist alone (Fig. 6*B*, ●) caused a similar reduction in ^{3}H incorporation into δVal-269 (2 cpm/pmol), and there

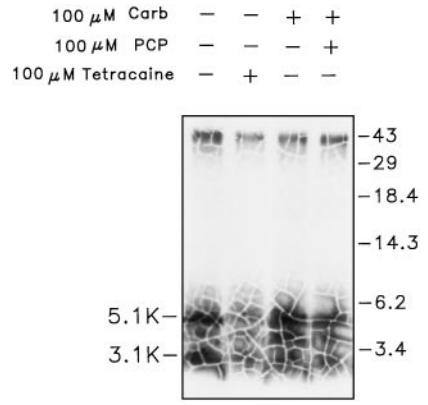

FIG. 4. **Trypsin digestion of δ-subunit from AChR photolabeled with [^{3}H]DAF in the presence and absence of carbamylcholine (*Carb*) and noncompetitive antagonists.** δ-Subunits, isolated from AChR-rich membranes labeled with [^{3}H]DAF under the four different conditions indicated (*top*), were digested with 20% (w/w) trypsin for 4 days. Aliquots of the digests (~5%) were fractionated by Tricine/SDS-PAGE and then subjected to fluorography for 8 weeks. The migration of prestained molecular weight standards are indicated on the *right*, and the relative molecular masses of the principal [^{3}H]DAF-labeled digestion products are shown on the *left*. The δT-5.1K band contains a fragment beginning at δMet-257 before M2 and extending through M3. The δT-3.1K fragment contains the M2 region alone, N terminus: δMet-257.

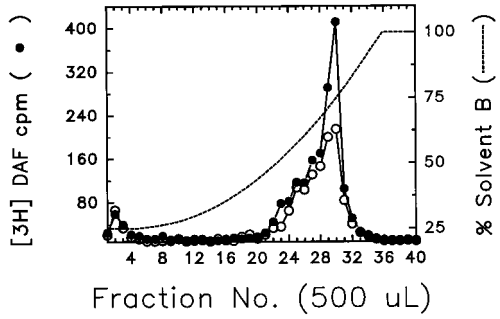

FIG. 5. **Reversed-phase HPLC purification of [^{3}H]DAF-labeled tryptic fragment δT-5.1K.** δT-5.1K isolated from tryptic digests of AChR δ-subunits (Fig. 4) was further purified by reversed-phase HPLC as described under "Experimental Procedures." The elution of [^{3}H]DAF-labeled peptides was determined by scintillation counting of aliquots (25 μl) of the collected fractions (●, ○). Elution profiles are shown for δT-5.1K material labeled in the absence of agonist but in the absence (●) or presence (○) of 100 μM tetracaine. Based upon the recovery of radioactivity, for each of the samples >90% of the material was recovered from the HPLC column.

the mass of the αTyr-401 peptide) and the amount of [^{3}H]DAF incorporation into αCys-412 (~4 cpm/pmol, Fig. 3*A* (cycle 12)), the 8 cpm release in cycle 12 of Fig. 3*B* must result from the α-subunit fragment. In contrast, the ^{3}H release in cycles 15, 17, 18, and 21 cannot result from the αTyr-401 peptide.

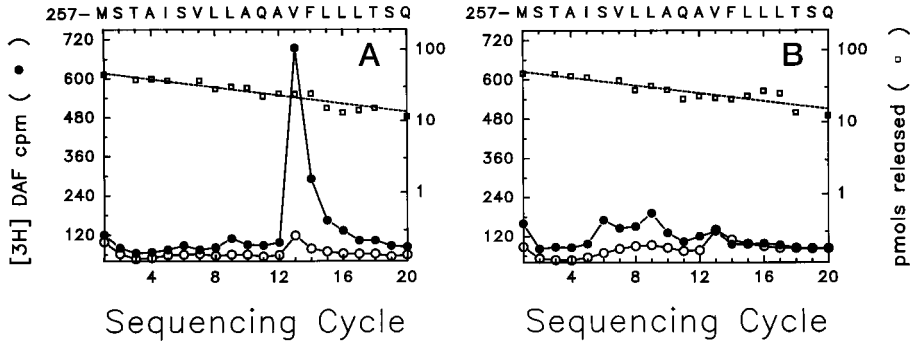

FIG. 6. **Radioactivity and mass release upon N-terminal sequence analysis of δ-T-5.1K.** δ-T-5.1K was isolated by Tricine/SDS-PAGE followed by reversed-phase HPLC (Fig. 5) and then subjected to automated Edman degradation, with 60% of each cycle analyzed for released ^{3}H (●, ○) and 30% for PTH-derivatives (□, with the *dashed lines* corresponding to the exponential decay fit of the amount of detected PTH-derivatives). The amino acid sequence of the sequenced peptide containing the M2 region is shown *above* each panel. *A*, ^{3}H release from δT-5.1K labeled in the absence of agonist (●, −/−), or in the absence of agonist but in the presence of 100 μM tetracaine (○, −/+). −/−: I_0 = 47 pmol; R = 93%; 15,000 cpm loaded/5,000 cpm remaining on filter. −/+: I_0 = 38 pmol; R = 94%; 9,000 cpm loaded/3,200 cpm remaining. *B*, ^{3}H release from δT-5.1K labeled in the presence of agonist (●, +/−) or in the presence of agonist and in the presence of 100 μM PCP (○, +/+). +/−: I_0 = 51 pmol; R = 93%; 13,700 cpm loaded/3,900 cpm remaining. +/+: I_0 = 57 pmol; R = 93%; 13,000 cpm loaded/3,500 cpm remaining.

was also a small but significant release of ^{3}H in cycles 6 and 9 that corresponds to [^{3}H]DAF incorporation into δSer-262 (1.9 cpm/pmol) and δLeu-265 (1.3 cpm/pmol) with similar efficiency as in δVal-269. Finally, in the presence of both agonist and 100 μM PCP, there was no detectable ^{3}H release in cycles 6 and 9, whereas release in cycle 13 was unaffected (Fig. 6*B*, ○).

In addition to δT-5.1K, sites of [^{3}H]DAF incorporation in δ-M2 were also revealed from the sequence analysis of δ-subunit tryptic fragments of 3.1 kDa (δ-T-3.1K; Fig. 4) and 7.4 kDa (data not shown). When purified by HPLC, the peak of ^{3}H for δT-3.1K (labeled in the absence of agonist) eluted earlier from the reversed-phase HPLC column (fractions 22–24) than did δT-5.1K. Sequence analysis revealed the presence of a primary sequence beginning at δMet-257 with a major site of ^{3}H release in cycle 13 (δVal-269). The molecular mass of δT-3.1K as well as its early elution from the reversed-phase column (52% organic) are consistent with this fragment containing the M2 but not the M3 region (*i.e.* Met-257–Arg-277). Identical amino termini (δMet-257) and ^{3}H release profile were observed upon sequencing δT-7.4K (HPLC fractions 29–31). These results not only confirm that δVal-269 is the site of incorporation of [^{3}H]DAF in δM2, they also confirm that both the labeled and unlabeled peptides are copurifying. This latter result is consistent with similar results observed using several different ligands and nearly identical purification steps (11, 13, 32).

Identification of the Sites of [^{3}H]DAF Incorporation in β-M2—In a manner similar to that for δ-subunit, the sites of [^{3}H]DAF photoincorporation in the M2 region of β-subunit were determined by digesting the subunit (~250 μg/labeling condition) with 20% (w/w) trypsin for 4 days. The digests from each of the four labeling conditions were then fractionated by Tricine/SDS-PAGE and a 7.2-kDa band (βT-7.2K), known to contain the M2–M3 region (13), was isolated (see under "Experimental Procedures"). When the gels were illuminated at 365 nm on a UV-light box, the βT-7.2K fragment, which migrates as a sharp band of ^{3}H in the fluorograph of an analytical Tricine/SDS-PAGE gel, migrated in an area of weak fluorescence between two strongly fluorescent bands of 10 and 5.5 kDas (data not shown). The material eluted from the βT-7.2K fragment was further purified by reversed-phase HPLC (Fig. 7), and for each labeling condition the majority of ^{3}H counts eluted in a peak centered at 84% solvent B. HPLC fractions 29–33 were pooled and sequenced (Fig. 8). In each of the four labeling conditions, sequence analysis revealed the presence of a single peptide beginning at βMet-249 at the N terminus of βM2 that was sequenced at similar efficiency and mass level for

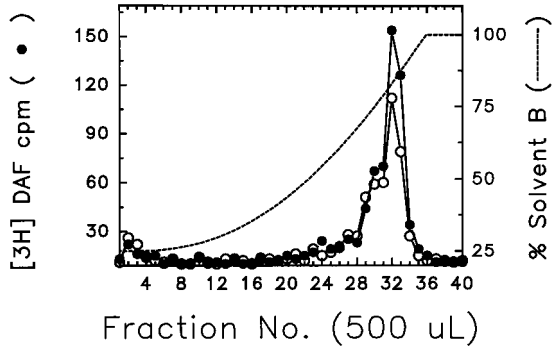

FIG. 7. **Reversed-phase HPLC purification of [^{3}H]DAF-labeled tryptic fragment βT-7.2K.** A 7.2-kDa molecular mass fragment isolated by Tricine/SDS-PAGE from tryptic digests of AChR β-subunit labeled under four different conditions material was then further purified by reversed-phase HPLC (see "Experimental Procedures"). The elution of [^{3}H]DAF-labeled peptides was determined by scintillation counting of aliquots (25 μl) of the collected fractions (●, ○). Elution profiles are shown for βT-7.2K material labeled in the absence of agonist but in the absence (●) or presence (○) of 100 μM tetracaine. Based upon the recovery of radioactivity, for each of the samples >90% of the material was recovered from the HPLC column.

each sample (see legend to Fig. 8). For the sample labeled in the absence of any ligands other than [^{3}H]DAF itself, the major release of ^{3}H release was in cycle 13, with lower release in cycle 9 (●, Fig. 8*A*). This pattern of release corresponds to [^{3}H]DAF incorporation into βLeu-257 (0.7 cpm/pmol) and βVal-261 (5.3 cpm/pmol) within β-M2. The presence of tetracaine (○, Fig. 8*A*) resulted in an approximately 95% reduction in the incorporation into βVal-261 (0.2 cpm/pmol). The addition of agonist (●, Fig. 8*B*) resulted in a substantial reduction in the amount of [^{3}H]DAF incorporated into βVal-261, although the extent of inhibition was difficult to quantify because that reduced release in cycle 13 was associated with a dramatic increase in ^{3}H release in cycles 9 and 10 that corresponds to increased incorporation of [^{3}H]DAF into βLeu-257 (2 cpm/pmol) and βAla-258 (~3 cpm/pmol). Interestingly, the presence of excess PCP (○, Fig. 8*B*) resulted in an 80% reduction in the amount of incorporation into βLeu-257 (0.4 cpm/pmol) but only a 50% reduction in the labeling of βAla-258 (1.5 cpm/pmol).

Identification of the Sites of [^{3}H]DAF Incorporation in α-M2—The α-subunits isolated from AChRs labeled under each of the four different conditions (~500 μg of α-subunit/labeling condition) were each digested with 1.5 units of endoproteinase Lys-C for 6 days. The digests were then resolved by Tricine/

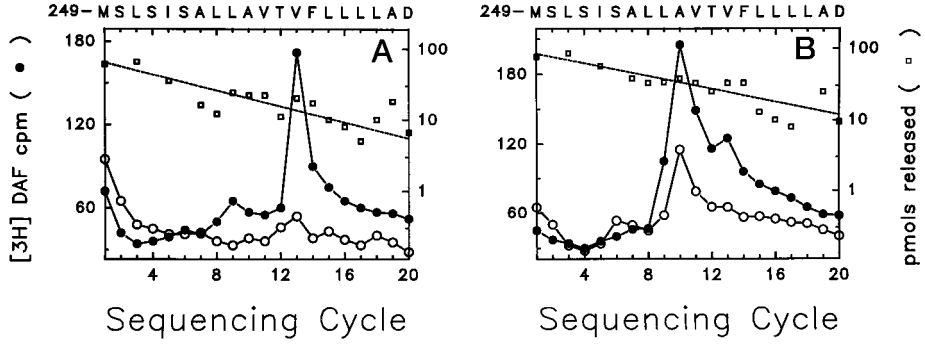

FIG. 8. **Radioactivity and mass release upon N-terminal sequence analysis of β-T-7.2K.** βT-7.2K was isolated by Tricine/SDS-PAGE followed by reversed-phase HPLC (Fig. 7) and then subjected to automated Edman degradation with 60% of each cycle analyzed for released ^{3}H (●, ○) and 30% for PTH-derivatives (□, with the *dashed lines* corresponding to the exponential decay fit of the amount of detected PTH-derivatives for the peptides containing M2). The amino acid sequence of the sequenced peptide containing the M2 region is shown *above* each panel. *A*, ^{3}H release from βT-7.2K labeled in the absence of agonist but in the absence (●, −/−) or presence (○, −/+) of 100 μM tetracaine. −/−: I_0 = 63 pmol; R = 88%; 9,200 cpm loaded/2,000 remaining on filter; −/+: I_0 = 61 pmol; R = 92%; 7,200 cpm loaded/1,400 cpm remaining). *B*, ^{3}H release from βT-7.2K labeled in the presence of agonist but in the absence (●, +/−) or presence of 100 μM PCP (○, +/+). +/−: I_0 = 70 pmol; R = 90%; 10,800 cpm loaded/2,400 cpm remaining. (+/+: I_0 = 70 pmol; R = 90%; 9,600 cpm loaded/2,900 cpm remaining.)

SDS-PAGE, and an approximately 10-kDa band (αK-10K), previously shown to contain the M2-M3 region (11), was excised (see "Experimental Procedures"). Inspection of the fluorogram of the gel of the analytical digests (Fig. 9) revealed that the αK-10K fragment migrated with lower mobility than the major radiolabeled band of 7.8 kDa that was also intensely fluorescent (not shown). When the material eluted from the αK-10K band was further purified by reversed-phase HPLC, for each labeling condition the majority of ^{3}H counts were in a peak centered at 78% solvent B. HPLC fractions 31–34 were pooled and sequenced (Fig. 10). For each sample the primary sequence began at αMet-243 before α-M2 (~25 pmol), and a secondary sequence beginning at αTyr-401 before M4 was present at ~8 pmol.[4] For all four of the samples, which correspond to each of the different labeling conditions, low level ^{3}H release was seen in cycles 12, 15, and 18. This pattern of release corresponds to that observed for nonspecific [^{3}H]DAF incorporation into α-M4 region, *i.e.* labeling of αCys-412, αMet-415, and αCys-418 (Fig. 3*A*).[4] For both of the α-K-10K samples labeled in the absence of agonist (with and without tetracaine), no other sites of ^{3}H release were evident (Fig. 10), a result that indicates that [^{3}H]DAF does not incorporate into α-M2. Had [^{3}H]DAF incorporated into αVal-255 in α-M2 at the same efficiency as it did into δVal-269, release of 180 cpm would be observed in cycle 13. For the αK-10K sample isolated from AChRs labeled in the presence of agonist, there was also ^{3}H release in cycles 6 and 9 at levels similar to cycle 12 (data not shown) that was eliminated (cycle 6) by the presence of PCP. Thus, in the presence of agonist there was low level labeling (~1 cpm/pmol) of αSer-248 and αLeu-251 as was seen for the equivalent amino acids in δ-M2 (Fig. 6*B*).

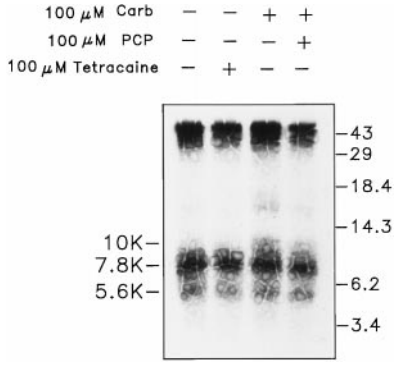

FIG. 9. **Endoproteinase Lys-C digestion of α-subunit from AChRs photolabeled with [^{3}H]DAF in the presence and absence of carbamylcholine and noncompetitive antagonists.** α-Subunit, which was isolated from AChR-rich membranes labeled with [^{3}H]DAF under the four different conditions indicated (*top*), was digested with 1.5 units of endoproteinase Lys-C for 6 days. Aliquots of the digests (~5%) were fractionated by Tricine/SDS-PAGE and then subjected to fluorography for 6 weeks. The migration of prestained molecular weight standards are indicated on the *right* and the relative molecular masses of the principal [^{3}H]DAF-labeled digestion products are shown on the *left*. The αK-7.8K fragment contained the M4 region, amino termini: αSer-388, αTyr-401. The αK-10K fragment contained a peptide beginning at αMet-243 before M2 and a peptide beginning at αTyr-401 before M4 (see Fig. 10).

DISCUSSION

The results presented here demonstrate that the uncharged hydrophobic compound 2-[^{3}H]diazofluorene ([^{3}H]DAF) photoincorporates in a specific and agonist-sensitive fashion into residues in the channel lining M2 region of the nicotinic AChR. In addition, [^{3}H]DAF photoincorporates in a agonist-insensitive manner into the M4 segment of each receptor subunit. Therefore, there exist two components to the labeling of the AChR by [^{3}H]DAF as follows: a nonspecific component consistent with incorporation into residues situated at the lipid-protein interface of the AChR, and a specific component, inhibitable by noncompetitive antagonists, sensitive to state-dependent transitions, and localized to residues within the ion channel. It is significant that even in the absence of agonist the specific photoincorporation of [^{3}H]DAF within δ- or β-M2 can be clearly revealed only during N-terminal sequence analyses of isolated peptides, since that component of the photolabeling is ≤20% of the total labeling at the level of isolated subunits or even of proteolytic fragments after fractionation by SDS-PAGE and reversed-phase HPLC (Figs. 5 and 7). Unlike [^{125}I]TID at micromolar concentrations for which the reaction with residues within M2 segments comprises 70% of the total labeling at the subunit level, for [^{3}H]DAF at micromolar concentrations labeling of δ-M2 does not predominate over labeling of residues in the M4 segments. For example, for M2 and M4 segments isolated from the same labeling experiment, the inhibitable ^{3}H incorporation in δVal-269 (7–8 cpm/pmol) is ~twice the level of nonspecific labeling in αCys-412 (3–4 cpm/pmol), the most

[4] Fragments containing α-M4 beginning at αTyr-401 and αSer-388 were found to be present at higher mass levels (40 pmol) in the material purified from the intensely fluorescent, radiolabeled 7.8-kDa fragment (αK-7.8K). Based upon the mass level of the αTyr-401 peptide in the αK-10K band (Fig. 10*A*), the ^{3}H release in cycle 12 would correspond to labeling of αCys-412 in M4 at a level (9 cpm/pmol) similar to that seen for labeling of αCys-412 (8 cpm/pmol) in the sequence analysis of the αK-7.8K band.

highly labeled residue in M4.

Characterization of [3H]DAF Labeling at the Lipid-Protein Interface—The majority of AChR labeling by [3H]DAF appears similar to the component of [125I]TID labeling which is inhibitable neither by agonist nor by an excess of non-radioactive TID and which is consistent with photoincorporation into lipid-exposed regions of the AChR (14–17). [3H]DAF incorporation into each AChR subunit M4 segment was determined under labeling conditions done in the absence and in the presence of 100 μM carbamylcholine. In either condition [3H]DAF reacted in α-M4 with His-408, Cys-412, Met-415, and Cys-418 (Fig. 3*A*); in β-M4 with Tyr-441, Phe-443, Phe-444, and Cys-447 (Fig. 3*B*); in γ-M4 with Cys-451 and Trp-453 (Fig. 3*C*). The low level of 3H release within δ-M4 allows only a tentative assignment for Met-458 (Fig. 3*D*). Although the isolation of M4 fragments by alternative digestion strategies would provide unambiguous proof that the observed 3H release originates from the observed M4 peptides, this is the expected result based upon previous studies with [125I]TID that establish that the labeled and unlabeled peptides coelute from the reversed-phase column (16, 17). It is also important to point out that due to the lags resulting from the ~90% repetitive yields inherent in the Edman degradation reaction, cycles that follow a labeled amino acid also contain prior PTH-derivatives and associated 3H. It is therefore difficult to detect the presence of labeled amino acids which immediately follow another labeled amino acid, particularly if the efficiency of incorporation into those residues is significantly lower. Without direct characterization of the 3H-labeled amino acids released in each cycle, one cannot determine whether some of the 3H release in cycles immediately following these labeled residues is due to amino acids which have also reacted with [3H]DAF.

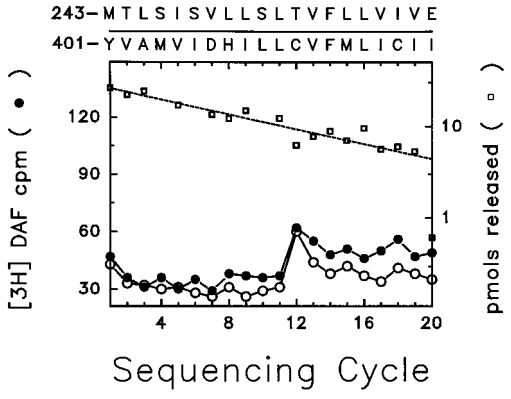

FIG. 10. **Radioactivity and mass release upon N-terminal sequence analysis of α-K-10K.** α-K-10K was isolated by Tricine/SDS-PAGE (Fig. 9) followed by reversed-phase HPLC (see "Experimental Procedures") and then subjected to automated Edman degradation with 60% of each cycle analyzed for released 3H (●, ○) and 30% for PTH-derivatives (□, with the *dashed lines* corresponding to the exponential decay fit of the amount of detected PTH-derivatives for the peptides containing M2). The amino acid sequences of the two primary peptides that were detected are both shown along the *top axis*. The sequence of the primary peptide began at αMet-243 and contained the M2 region, whereas the secondary sequence began at αTyr-401 and contained M4. The profile of 3H release is shown for αK-10K labeled in the absence of agonist (●, −/−) or in the absence of agonist and in the presence of 100 μM tetracaine (○, −/+). (−/− (αMet-243): I_0 = 25 pmol; R = 91%; (αTyr-401): I_0 = 7.8 pmol; R = 93%; 14,600 cpm loaded/3,500 cpm remaining on filter after 20 cycles. −/+ (Met-243): I_0 = 25 pmol; R = 91%; (αTyr-401): I_0 = 8.7 pmol; R = 88%; 15,700 cpm loaded/3,400 cpm remaining on filter after 20 cycles.)

Residues incorporating [3H]DAF are summarized in Fig. 11 where M4 segments are modeled as α-helices and residues previously shown to react with [125I]TID (17) are indicated with an *asterisk*. Both [125I]TID and [3H]DAF are hydrophobic compounds that partition efficiently into *Torpedo* membranes. In addition, both compounds incorporate via a UV-induced reactive carbene. It is therefore not surprising that many of the same residues in the M4 regions of each of the AChR subunits are labeled by both compounds. However, each of these compounds is structurally as well as photochemically unique, with TID forming a singlet carbene (20) and DAF a carbene with substantial triplet character (21, 22). Interestingly, αHis-408, βPhe-443, and γTrp-453 are labeled by [3H]DAF but not [125I]TID. As previously noted for the labeling pattern of [125I]TID (17), positional effects rather than intrinsic reactivities appear to have a more dominant effect on the observed [3H]DAF labeling pattern. For example in α-M4 there is an approximately 3-fold difference in the efficiency of incorporation between αCys-412 (3.7 cpm/pmol) and αCys-418 (1.2 cpm/pmol), and incorporation into βTyr-441 (1.3 cpm/pmol), the residue equivalent to αCys-412, is 3-fold higher than that of βCys-447 (~0.4 cpm/pmol), the position equivalent to αCys-418, even though cysteine is likely to have substantially greater intrinsic reactivity than tyrosine. Within γ- and δ-subunits [3H]DAF incorporation is particularly restricted, with no incorporation detectable C-terminal to the positions equivalent to αCys-412. However, the lack of other identifiable labeled residues in these M4 segments may simply reflect the low level radiolabeling attainable with [3H]DAF at 1.4 Ci/mmol, and further studies using [3H]DAF of higher radiochemical specific activity will be necessary to clarify whether or not residues such as γPhe-459, γSer-460, or δMet-465 are labeled.

The simplest interpretation of the periodicity of [3H]DAF-

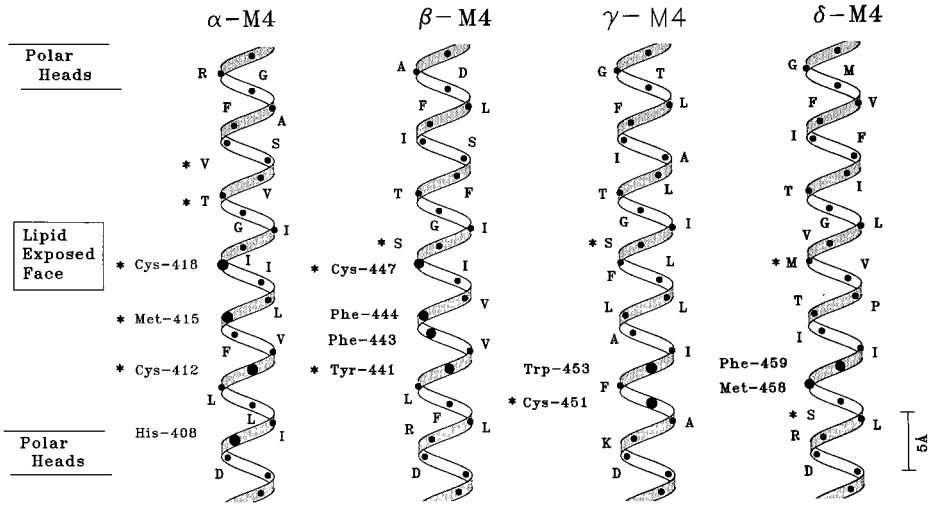

FIG. 11. **Helical representations of the α-, β-, γ-, and δ-subunit M4 regions.** Helical representations of the α-, β-, γ-, and δ-subunit M4 regions. [3H]DAF-labeled amino acid residues are indicated along the *left side* of the helix along with the location of the labeled amino acid in the subunit primary sequence. *Asterisks* denote residues that were previously shown to be labeled by [125I]TID (16, 17). Helices are oriented with N termini at the bottom to reflect the extracellular location of the carboxyl termini (46).

labeled residues within the M4 segments of each subunit is that each of these regions possesses α-helical secondary structure. Within α-M4 the labeled amino acids would lie on a broadly defined face of an α-helix distributed over four consecutive turns, and when combined with the results for [^{125}I]TID (17), labeled residues extend over 6 helical turns, spanning a distance of ~25 Å (Fig. 11). In contrast, the distribution of [^{3}H]DAF-labeled residues in α-M4 is inconsistent with labeling of a single face of a β-strand, since three labeled residues (His-408, Cys-412, and Cys-418) would lie on one face and Met-415 would lie on the other. Within β-M4, labeled residues would extend over three helical turns. The limited labeling in γ- and δ-M4 precludes assignment of their secondary structure.

Identification of the residues and the corresponding face of the M4 helices that are in contact with the lipid bilayer provides an extra measure of importance to several recent structure-function studies. αCys-418 is labeled nonspecifically by [^{125}I]TID (16, 17), by [^{125}I]iodonaphthylazide (33), and by [^{3}H]DAF, and therefore, this position is in all probability exposed to the lipid bilayer. Interestingly, mutation of αCys-418 to tryptophan results in a 28-fold increase in channel open time, with no effect on channel conductance (34). Similarly, Bouzat *et al.* (35) have shown that in the fetal mouse AChR γLeu-440 and γMet-442 contribute to long duration open channel events. Both residues are by homology located on the lipid-exposed face of γ-M4, with γLeu-440 equivalent to *Torpedo* αCys-412 (as well as to γTrp-453). The obvious implication for both these studies is that the interactions of regions of the AChR with the lipid bilayer play an important role in the determination of the kinetics of channel gating.

Characterization of [^{3}H] DAF Labeling in the Channel—In the absence of agonist, [^{3}H]DAF labels within M2 segments two homologous aliphatic residues, βVal-261 and δVal-269. Incorporation into these residues is reduced greater than 90% by the addition of an excess of tetracaine, which binds within the channel in the absence of agonist (30). Surprisingly, in the absence of agonist, no [^{3}H]DAF incorporation was detected in α-M2. It is also striking that the incorporation of [^{3}H]DAF into δVal-269 occurred five times more efficiently than into βVal-261. The preferential incorporation into δVal-269 cannot be easily explained by differences in amino acid side chain reactivities, since a valine is present at that position in all three subunits (α, β, δ). Thus [^{3}H]DAF bound within the ion channel must be oriented with its photoreactive diazo group facing the side chain of δVal-269. This selective orientation is then a consequence of the asymmetry of the [^{3}H]DAF molecule and of the pore of the ion channel itself. The lack of incorporation into α-M2 and the less efficient incorporation into β-M2 compared with δ-M2 reflects the arrangement of subunits in the pentameric receptor: α-γ-α-δ-β (11, 36, 38). Only by determining if [^{3}H]DAF also reacts with γ-M2 can it be determined whether [^{3}H]DAF can exist in the channel in more than one possible orientation.

As is illustrated in Fig. 12, the structure of [^{3}H]DAF, the position of its photoreactive diazo group, and its selective incorporation in the absence of agonist into δVal-269 and βVal-261 are consistent with a constriction in the closed ion channel located approximately one turn of an α-helix lower at or near δLeu-265 (position 9). White and Cohen (13) reached essentially this same conclusion based on the incorporation of [^{125}I]TID into residues at positions 9 and 13 of the M2 region. Taken together these two reports reinforce this conclusion as well as the supposition that this restriction might also provide a barrier to the passage of ions in the closed ion channel.

Further evidence in support of the proposition that a restriction in the channel exists at or around the leucine residues at position 9 comes from several different investigations. In the recent three-dimensional structures of the AChR derived from electron micrographic image analysis, within the transmembrane portion of the AChR rod-like structures can be seen forming the lining of channel pore (4, 12). These rods, which are interpreted as representing the M2 segments in an α-helical conformation, are kinked inward toward the central axis at about their midpoints. Alignment of the three-dimensional densities (*i.e.* rods) with the amino acid sequence of M2 suggested that the ring of leucine residues at position 9 project from the kink and that the association of the leucine side chains could form a hydrophobic ring, providing a barrier to the passage of ions. In the presence of agonist, small rotational motions in the M2 helices would disrupt the association and allow ion permeation (4). A number of electrophysiological investigations have focused on the functional consequences of substitutions of the leucines at position 9. For the α7 neuronal AChR expressed in oocytes, mutations to several different amino acids, including serine, result in large leftward shifts of the dose response for acetylcholine and in a reduction of the kinetics of desensitization (39). In the muscle-type AChR, for each leucine to serine mutation the dose response is shifted to the left by about an order of magnitude (40, 41). Thus, hydrophobic interactions between the leucine residues play an important role in AChR gating (see also Refs. 38 and 42).

A very different model of the structure of the closed channel results from studies utilizing cysteine-reactive methane thiosulfonate derivatives as reactive probes of residues in M2 that have been mutated to cysteines (43). Since in the absence of agonist residues lower in the channel than position 9, and even as low as −1, were still accessible to the probes, it was suggested that the permeability barrier in the closed channel must be located outside the M2 region. Further studies will be required to determine unambiguously the permeability barrier to hydrated Na^+ in the closed channel.

In the presence of agonist, [^{3}H]DAF labels a different set of

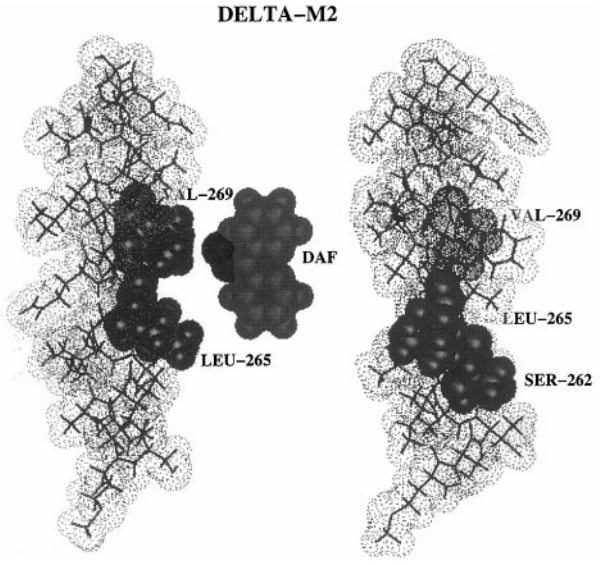

FIG. 12. **Corey-Pauling-Koltun models of the δ-M2 helix with DAF.** Corey-Pauling-Koltun helical representation of the δ-M2 region drawn to scale with a (*space-filled*) DAF molecule. *Left*, DAF, with its linear diazo group only approximated (*shaded*), is shown facing the δVal-269 side chain labeled by [^{3}H]DAF in the absence of agonist. The model illustrates that a phenyl ring of diazofluorene (in this orientation) is approximately in register with δLeu-265, located one turn of an α-helix lower in the channel than δVal-269. *Right*, the Corey-Pauling-Koltun helix is rotated to illustrate δVal-269 labeled by [^{3}H]DAF in the absence of agonist (resting state) and δSer-262 and δLeu-265 labeled in the presence of agonist (desensitized state).

residues in the M2 region. In the α- and δ-subunits, a homologous set of residues are labeled at positions 6 and 9 (αSer-248, αLeu-251, δSer-262, and δLeu-265), whereas in β-M2 residues at positions 9 and 10 are labeled (βLeu-257 and βAla-258). It is striking that the labeling of δ-M2 in the presence of agonist (desensitized state) was 10-fold less efficient than the labeling in the absence of agonist (Fig. 6). For [^{125}I]TID the agonist-induced decrease in the effiency of photoincorporation was observed at positions 9 and 13 in M2 segments of each subunit (13). For neither probe can this decrease in labeling be simply attributed to any differences in binding affinity. [^{125}I]TID binds to the channel with micromolar affinity both in the presence and absence of agonist (15), and [^{3}H]DAF also inhibits the binding of [^{3}H]tetracaine in the absence of agonist and [^{3}H]PCP in the presence of agonist with similar IC_{50} values (Fig. 1).[2] One explanation is that in the presence of agonist, some molecule near the binding site, perhaps water, is scavenging the photoactivated species (15, 13). However, in the case of [^{3}H]DAF, this dramatic agonist-induced decrease in the efficiency of photoincorporation is only observed in δ-M2. In β-M2 [^{3}H]DAF photoincorporates into different residues in the two states but with similar efficiencies. An alternative hypothesis is that for either [^{125}I]TID or [^{3}H]DAF the efficiency of photoincorporation is extremely sensitive to the environment around the binding site. Subtle differences in the positions of amino acid side chains that have no net effect on the overall binding affinity may dramatically effect how the photogenerated reactive carbene inserts. An absence of water in the closed, desensitized channel is also consistent with a characterization of the molecular environment of the channel as being very hydrophobic and with a low dielectric constant (44).

The residues labeled by [^{3}H]DAF in the presence of agonist would be located one or two turns of an α-helix lower in the channel than the residues labeled in the absence of agonist. The redistribution in labeled residues strongly supports previous observations of an agonist-induced rearrangement of the M2 helices (13). On the other hand, the redistribution of labeled residues is relatively small. In fact, residues labeled by [^{3}H]DAF in the presence of agonist (*i.e.* δLeu-265 at position 9) are also strongly labeled by [^{125}I]TID in the absence of agonist (13). In addition, site-directed mutagenesis experiments reveal that hydrophobic residues at position 10 of the M2 helix stabilize the binding of QX-222 in the open channel state (45). These facts taken together suggest that the changes in the structure of the channel between the closed, open, and desensitized states may be quite subtle. Gross movements of the M2 helices such as significant changes in the degree of tilt may be unnecessary. Small rotational motions in the helices that serve to draw the leucine side chains away from the central axis, such as those proposed by Unwin (4), may better describe the experimental data. In the absence of agonist there is a small amount of [^{3}H]DAF incorporation into βLeu-257 in β-M2, whereas in the presence of agonist there is incorporation into βLeu-257 and βAla-258. One interpretation is that this provides evidence of a small rotational movement in the β-M2 helix between the resting and desensitized state.

In summary, our results demonstrate that [^{3}H]DAF labels the channel-forming M2 region of AChR subunits. In the absence of agonist, [^{3}H]DAF specifically labels homologous aliphatic residues at position 13 in the β- and δ-subunit M2 region and does not react with the corresponding Val in α-subunit. In the presence of agonist, there is a redistribution in the labeled residues. In α-M2 and δ-M2 residues at positions 6 and 9 are labeled, and in β-M2, residues at positions 9 and 10 are labeled. The redistribution of labeled residues argues in favor of a state-dependent rearrangement of the M2 segments (Fig. 12).

Acknowledgment—We thank Martin Gallagher for helpful comments and suggestions.

REFERENCES

1. Karlin, A. (1993) *Curr. Opin. Neurobiol.* **3,** 299–309
2. Galzi, J.-L., and Changeux, J.-P. (1995) *Neuropharmacology* **34,** 563–582
3. Hucho, F., Tsetlin, V. I., and Machold, J. (1996) *Eur. J. Biochem.* **239,** 539–557
4. Unwin, N. (1995) *Nature* **373,** 37–43
5. Peper, K., Bradley, J., and Dreyer, F. (1982) *Physiol. Rev.* **62,** 1271–1340
6. Giraudat, J., Dennis, M., Heidmann, T., Chang, J., and Changeux, J. P. (1986) *Proc. Natl Acad. Sci. U. S. A.* **83,** 2719–2723
7. Giraudat, J., Dennis, M., Heidmann, T., Haumont, P.-Y., Lederer, F., and Changeux, J.-P. (1987) *Biochemistry* **26,** 2410–2418
8. Giraudat, J., Galzi, J.-L., Revah, F., Changeux, J.-P., Haumont, P.-Y., and Lederer, F. (1989) *FEBS Lett.* **253,** 190–198
9. Revah, F., Galzi, J.-L., Giraudat, J., Haumont, P.-Y., Lederer, F., and Changeux, J.-P. (1990) *Proc. Natl. Acad. Sci. U. S. A.* **87,** 4675–4679
10. Hucho, F. (1986) *Eur. J. Biochem.* **158,** 211–226
11. Pedersen, S. E., Sharp, S. D., Liu, W.-S., and Cohen, J. B. (1992) *J. Biol. Chem.* **267,** 10489–10499
12. Unwin, N. (1993) *J. Mol. Biol.* **229,** 1101–1124
13. White, B. H., and Cohen, J. B. (1992) *J. Biol. Chem.* **267,** 15770–15783
14. White, B. H., and Cohen, J. B. (1988) *Biochemistry* **27,** 8741–8751
15. White, B. H., Howard, S., Cohen, S. G., and Cohen, J. B. (1991) *J. Biol. Chem.* **266,** 21595–21607
16. Blanton, M. P., and Cohen, J. B. (1992) *Biochemistry* **31,** 3738–3750
17. Blanton, M. P., and Cohen, J. B. (1994) *Biochemistry* **33,** 2859–2872
18. Pradhan, D., and Lala, A. K. (1987) *J. Biol. Chem.* **262,** 8242–8251
19. Lala, A. K., and Raja, S. M. (1995) *J. Biol. Chem.* **270,** 11348–11357
20. Brunner, J. (1989) *Methods Enzymol.* **172,** 629–687
21. Anjaneylu, P. S., and Lala, A. K. (1984) *Indian J. Chem.* **23,** 802–807
22. Tomioka, H., Kawasaki, H., Kobayashi, N., and Hirai, K. (1995) *J. Am. Chem. Soc.* **117,** 4493–4498
23. Laemmli, U. K. (1970) *Nature* **227,** 680–685
24. Middleton, R. E., and Cohen, J. B. (1991) *Biochemistry* **30,** 6987–6997
25. Cleveland, D. W., Fischer, S. G., Kirschner, M. W., and Laemmli, U. K. (1977) *J. Biol. Chem.* **252,** 1102–1106
26. Pedersen, S. E., Dreyer, E. B., and Cohen, J. B. (1986) *J. Biol. Chem.* **261,** 13735–13743
27. Hager, R. A., and Burgess, R. R. (1980) *Anal. Biochem.* **109,** 76–86
28. Schagger, H., and von-Jagow, G. (1987) *Anal. Biochem.* **166,** 368–379
29. Cohen, J. B., Medynski, D. C., and Strnad, N. P. (1985) in *Effects of Anesthesia* (Covino, G., Fozzard, H. A., Rehder, K., and Strichartz, G., eds) pp. 53–63, American Physiological Society, Bethesda
30. Gallagher, M. J., and Cohen, J. B. (1994) *Biophys. J.* **66,** 212A (abstr.)
31. Heidmann, T., Oswald, R. E., and Changeux, J.-P. (1983) *Biochemistry* **22,** 3112–3127
32. Blanton, M. P., Li, Y., Stimson, E. R., Maggio, J. E., and Cohen, J. B. (1994) *Mol. Pharmacol.* **46,** 1048–1055
33. Blanton, M. P., and Cohen, J. B. (1993) *Biophys. J.* **64,** 322A (abstr.)
34. Lee, Y.-H., Li, L., Lasalde, J., Rojas, L., McNamee, M., Ortiz-Miranda, and S. I., and Pappone, P. (1994) *Biophys. J.* **66,** 646–653
35. Bouzat, C., Bren, N., and Sine, S. M. (1994) *Neuron* **13,** 1395–1402
36. Blount, P., and Merlie, J. P. (1989) *Neuron* **3,** 5349–5357
37. Deleted in proof
38. Kearney, P. C., Zhang, H., Zhong, W., Dougherty, D. A., and Lester, H. A. (1996) *Neuron* **17,** 1221–1229
39. Revah, F., Bertrand, D., Galzi, J.-L., Devillers-Thiry, A., Mulle, C., Hussy, N., Bertrand, S., Ballivet, M., and Changeux, J.-P. (1991) *Nature* **352,** 846–849
40. Labarca, C., Nowak, M. W., Zhang, H., Tang, L., Deshpande, P., and Lester, H. A. (1995) *Nature* **376,** 514–516
41. Filatov, G. N., and White, M. M. (1995) *Mol. Pharmacol.* **48,** 379–384
42. Lester, H. A. (1997) *Harvey Lect.* **91,** 79–99
43. Akabas, M. H., Kaufmann, C., Archdeacon, P., and Karlin, A. (1994) *Neuron* **13,** 919–927
44. Palma, A. L., and Wang, H. H. (1991) *J. Membr. Biol.* **122,** 143–153
45. Charnet, P., Labarca, C., Leonard, R. J., Vogelaar, N. J., Czyzyk, L., Gouin, A., Davidson, N., and Lester, H. A. (1990) *Neuron* **2,** 87–95
46. DiPaola, M., Czajkowski, C., and Karlin, A. (1989) *J. Biol. Chem.* **264,** 15457–15463